

Estimating local interaction from spatiotemporal forest data, and Monte Carlo bias correction

Akiko Satake^{a,b,*}, Yoh Iwasa^a, Hiroshi Hakoyama^c, Stephen P. Hubbell^d

^aDepartment of Biology, Faculty of Sciences, Kyushu University, Fukuoka 812-8581, Japan

^bDepartment of Entomology, 505 ASI Building, The Pennsylvania State University, University Park, PA 16802, USA

^cHokkaido National Fisheries Research Institute, Katsurakoi 116, Kushiro 085-0802, Japan

^dDepartment of Botany, Georgia University, Athens, GA 30602, USA

Received 30 December 2002; accepted 3 September 2003

Abstract

We point out a general problem in fitting continuous time spatially explicit models to a temporal sequence of spatial data observed at discrete times. To illustrate the problem, we examined the continuous time Markov model for forest gap dynamics. A forest is assumed to be apportioned into discrete cells (or sites) arranged in a regular square lattice. Each site is characterized as either a gap or a non-gap site according to the vegetation height of trees. The model incorporates the influence of neighboring sites on transition rate: transition rate from a non-gap to a gap site increases linearly with the number of neighbors that are currently in the gap state, and vice versa. We fitted the model to the spatiotemporal data of canopy height observed at the permanent plot in Barro Colorado Island (BCI). When we used the approximate maximum likelihood method to estimate the parameters of the model, the estimated transition rates included a large bias—in particular, the strength of interaction between nearby sites was underestimated. This bias originated from the assumption that each transition between two observation times is independent. The interaction between sites at local scale creates a long chain of transitions within a single census interval, which violates the independence of each transition. We show that a computer-intensive method, called Monte Carlo bias correction (MCBC), is very effective in removing the bias included in the estimate. The global and local gap densities measuring spatial aggregation of gap sites were computed from simulated and real gap dynamics to assess the model. When the approximate likelihood estimates were applied to the model, the predicted local gap density was clearly lower than the observed one. The use of MCBC estimates, suggesting a strong interaction between sites, improved this discrepancy.

© 2003 Elsevier Ltd. All rights reserved.

Keywords: Gap dynamics; Markov model; Maximum likelihood method; Bias correction; Parameter estimation; Spatial data

1. Introduction

Recent rapid development of remote sensing technology has greatly enhanced the availability of high-resolution map data of ecosystems in digital forms. Long-term forest research plots also provide spatial data indicating the location, size, and height of each individual tree in a forest ecosystem over a number of years. Spatially explicit dynamic models are becoming a standard tool for analysing a temporal sequence of

spatial data (e.g. Law et al., 1997; Alonso and Solé, 2000; many chapters in Dieckmann et al., 2000). Model fitting based on those spatial data should give us an opportunity to estimate parameter values which otherwise can be obtained by costly experimental manipulations. This procedure also allows us to select the most suitable model among alternatives once a sufficient amount of data becomes available. Considering the increase in the availability of spatial data, the development of techniques for model selection and parameter estimation using these data is very important in ecology.

One of the simplest examples of ecosystem models with explicit spatial structure is a continuous-time Markov model for the gap dynamics in a neotropical forest studied by Kubo et al. (1996). Gaps are openings created in a forest canopy—for example, by tree falls.

*Corresponding author. Department of Biology, Faculty of Sciences, Kyushu University, Fukuoka 812-8581, Japan. Tel.: +81-92-642-2638; fax: +81-92-642-2645.

E-mail address: satake@bio-math10.biology.kyushu-u.ac.jp (A. Satake).

Mechanisms of creation and expansion of canopy gaps have attracted much attention by forest ecologists, because gap disturbances followed by recruitment from seedlings provide important ways by which most tree species maintain their representation in closed canopy forests (Hubbell et al., 1999; Brokaw and Busing, 2000; Schnitzer et al., 2000; Schnitzer and Carson, 2001; Grau, 2002). In Kubo et al. (1996), a forest is assumed to be composed of many sites arranged on a regular square lattice. Each site is characterized as either a gap or a non-gap site according to the vegetation height, and changes its state randomly between the two. In the model, gap formation rate, the rate of transition from a non-gap to a gap, increases linearly with the number of neighbors that are currently in the gap state. This suggests that trees adjacent to existing gaps suffer a greater risk of falling than those surrounded by tall vegetation, presumably because of higher exposure to wind. An enhanced rate of gap formation near pre-existing gaps has been observed in various forests, including subalpine spruce-fir forest (Lawton and Putz, 1988), deciduous old-growth forest (Runkle, 1984), and tropical forest (Hubbell and Foster, 1986; Kanzaki et al., 1994).

When the spatially explicit model is fitted to a temporal sequence of spatial data observed at discrete points in time, parameters of the model may be estimated by a simple regression or by an approximate maximum likelihood method, as was done in Kubo et al. (1996). Both of these methods assume that any two transition events are independent. In this paper, we show that, in the continuous-time model, such an assumption may cause considerable bias in estimating parameters—it is particularly likely when long chains of transitions caused by short-range interaction (for example, multiple gap formations caused by gap expansion of pre-existing gaps) have occurred between two observations. This bias exists in estimating the strength of local interaction based on any spatial data in which multiple clumped transitions occur between two successive census times.

We show that the bias can be completely removed by applying a computer-intensive method called Monte Carlo bias correction (MCBC) proposed by Hakoyama and Iwasa (2000a,b). To elucidate the use of MCBC, we investigated the temporal sequence of gap dynamics data observed at the 50 ha permanent plot in neotropical forest in Barro Colorado Island, Panama. When transition rates were estimated by applying the approximate maximum likelihood method, estimates included a considerable bias—in particular, the strength of interaction between nearby sites (i.e. gap/non-gap expansion rate) was underestimated. We first tried a simple intuitive method to remove the bias, and show that the method cannot completely remove the bias. We then applied the MCBC method and showed that it is very

effective in eliminating the bias, resulting in estimates showing stronger interaction between sites than the approximate maximum likelihood estimates.

2. Model and methods

2.1. A lattice model for forest gap dynamics

We investigate the spatial data of canopy height observed at the permanent plot in Barro Colorado Island (BCI), Panama. The forest was apportioned into discrete cells (or sites) of size $5 \times 5 \text{ m}^2$ arranged in a square lattice (Hubbell and Foster, 1986). Since the lattice includes 101×201 grids, the total area is about 50 ha. In the original data, sites were classified into six classes according to the vegetation height: 0–2, 2–5, 5–10, 10–20, 20–30, and more than 30 m. Here, we simply classify the sites into “gap” sites (0) with the vegetation height less than 20 m and “non-gap” sites (+) with the vegetation height taller or equal to 20 m, as in Kubo et al. (1996). An operational definition of gaps and non-gaps is given by choosing a certain threshold height and by regarding a site as a gap site if the height of trees is lower than that level. For instance, 20 m (Runkle, 1984; Hubbell and Foster, 1986), 10 m (Runkle, 1981; Yamamoto, 1993), or 3 m (Lawton and Putz, 1988) are chosen depending on the height of mature canopy trees in forests. The map data were provided over 11 years from 1983 to 1993.

By comparing spatial distributions of gaps and non-gaps observed in two consecutive years, we can detect the locations where transitions have occurred (Fig. 1). Red squares indicate the sites that experienced the transition from a non-gap to a gap ($+ \rightarrow 0$), which is called “gap formation”. Yellow squares in turn are the sites that experienced the transition from a gap to a non-gap ($0 \rightarrow +$), which is called “gap closure”.

Transition rate of a site depends strongly on its local environment. Fig. 2a illustrates the fraction of non-gap sites that experienced transition to gap sites by the following census time. We here classified the non-gap sites according to the number of gap sites in the neighborhood, in which each site has eight neighbors (Moore neighborhood). We excluded sites at the edge of the study plot. Fig. 2a demonstrates that the gap formation rate increases with the number of gap sites in the neighborhood. Non-gap sites surrounded by many gaps were more likely to become gaps than those which had no gap in their neighborhood, indicating a “gap expansion” of pre-existing gaps. Fig. 2b illustrates the rate for gap closure, the transition from gap sites to non-gap sites. The gap closure rate in turn increased with the number of non-gap sites in the neighborhood.

Kubo et al. (1996) studied a continuous-time Markov model to describe the spatiotemporal pattern of gap and

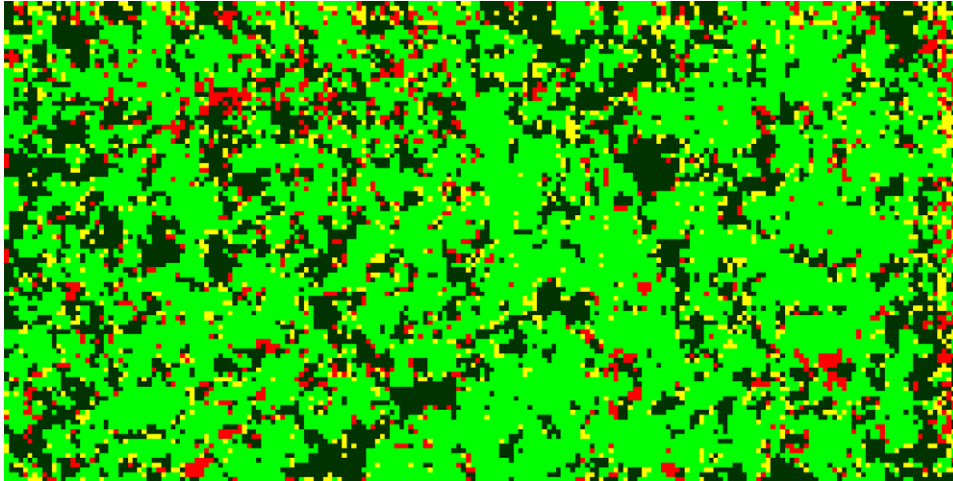


Fig. 1. Map of Barro Colorado Island (BCI). Each square corresponds to $5 \times 5 \text{ m}^2$ grid in the 50 ha plot. Green squares are non-gap sites (with the vegetation height taller than or equal to 20 m) and gray squares are gap sites (with the vegetation height less than 20 m) both in 1983 and in 1984. Red squares are gap formation sites that showed transition from non-gaps to gaps between 1983 and 1984. Yellow squares are gap closure sites that experienced transition from gaps to non-gaps within a year.

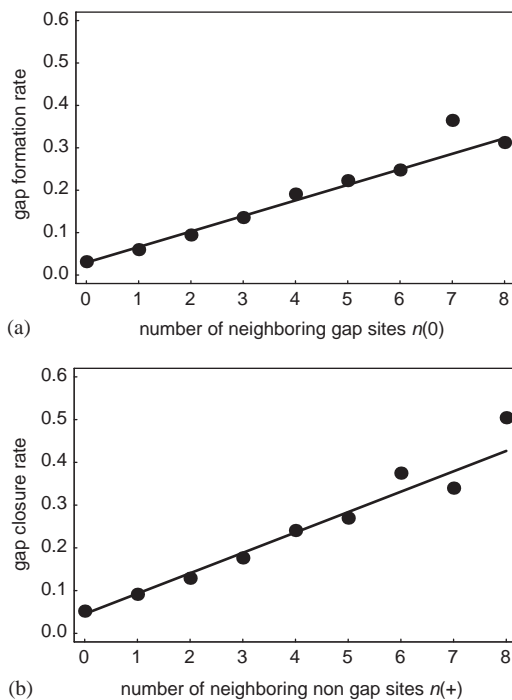


Fig. 2. Gap formation and closure rate. (a) Gap formation rate. Solid circles are the fraction of non-gap sites that experienced transition to gap sites before the following census time. Horizontal axis is the number of gap sites in the neighborhood of the focal non-gap site. Regression line is $y = 0.037n(0) + 0.029$ (a solid line). (b) Gap closure rate. Solid circles are the fraction of gap sites that made transition to non-gap sites within a year. The regression line is $y = 0.048n(+) + 0.045$ (a solid line). Moore neighborhood ($z = 8$) was adopted.

non-gap sites. They assumed that the gap formation and the gap closure are dependent on the status of neighboring sites. Let the number of neighboring gaps

or non-gaps be $n(0)$ and $n(+)$. They satisfy $n(0) + n(+) = z$, in which z is the number of neighbors ($z = 4$ for Neumann neighborhood and $z = 8$ for Moore neighborhood). The probability of gap formation ($+ \rightarrow 0$) and that of gap closure ($0 \rightarrow +$) in a short time interval of length Δt are

Gap formation ($+ \rightarrow 0$):

$$\text{with probability} \left[d + \frac{\delta}{z} n(0) \right] \Delta t, \quad (1a)$$

Gap closure ($0 \rightarrow +$):

$$\text{with probability} \left[b + \frac{\beta}{z} n(+) \right] \Delta t, \quad (1b)$$

where d , δ , b , and β are constants. In Eq. (1a), transition rate for each site is the sum of two terms, one independent of the neighbors (d) and the second proportional to the number of neighboring gap sites ($\delta n(0)/z$). We call d and δ the “independent” and “expansion” rate of gap formation. In a similar way, gap closure rate in Eq. (1b) is the sum of neighbor-independent and expansion rate of gap closure, which are given by two parameters, b and β respectively. Since it is known that disturbances and subsequent gap formation occur in all seasons in both tropical and temperate forests (Denslow, 1987; Runkle, 1989), a continuous-time model is more realistic than the discrete-time model where the clear seasonality in gap formation is assumed.

2.2. Bias in parameter estimation by simple fitting

We may plot the fraction of sites that experienced a transition within a year against the number of surrounding gaps (see Fig. 2). A simple way to estimate the rate

parameters (the gap formation or the gap closure rate) is to find the regression line fitted to these data using a simple least-squares estimate. A more desirable procedure to obtain a regression line would be to use the approximate maximum likelihood estimate explained in Appendix A. These methods are based on the simplifying assumption that the transitions experienced by different sites are independent of each other, and that the realized transition follows a binomial distribution with the mean rate given by Eq. (1) for each $n(0)$ and $n(+)$. The estimated transition rates using the approximate maximum likelihood method and resultant linear functions of the number of neighboring gap sites are indicated as solid lines in Fig. 2. The regression lines calculated by simple least-squares method were very close to those obtained by the approximate maximum likelihood method.

However, both of these methods include considerable bias in estimating transition rates. To illustrate this, first, we chose a “true” transition rule specified by a set of parameters, gap formation and closure rate. Second, using the true rule, we generated a number of realizations of the continuous-time Markov model (Eq. (1)) by independent Monte Carlo simulations. To remove the effect of edges, we adopted a periodic boundary condition, i.e. the lattice of a torus shape (the rightmost column is the nearest neighbor of the leftmost column, and the top row is nearest neighbor of the bottom row). As an initial condition for each run, we chose the canopy data observed at the BCI plot in 1983. Third, we calculated the approximate maximum likelihood estimate from each realization generated by independent run. In counting the fraction of transition sites from simulated map data, we removed sites at the boundary of the lattice.

The thick solid line in Fig. 3a is the true transition rule for gap formation that was used to generate the artificial spatial data, and the circles and bars indicate the mean and standard error of the fraction of transitions observed in those data. The approximate maximum likelihood estimate, given by a dotted line, fits well to the observed fraction of transitions. However, it is clearly different from the true transition rule (thick solid line), tending to underestimate the slope (δ) and overestimate the intercept (d).

In Fig. 3b, we plotted the approximate maximum likelihood estimates on a $d - \delta$ plane. A solid circle indicates the true transition parameters for gap formation ($d = 0.027$, $\delta = 0.36$) used in the Monte Carlo simulation. The approximate maximum likelihood estimates calculated for all realizations are indicated by black dots with their average (an open circle). They clearly show smaller δ and larger d than the true values, implying a significant bias of underestimation of δ (expansion rate) but overestimation of d (neighbor-independent rate).

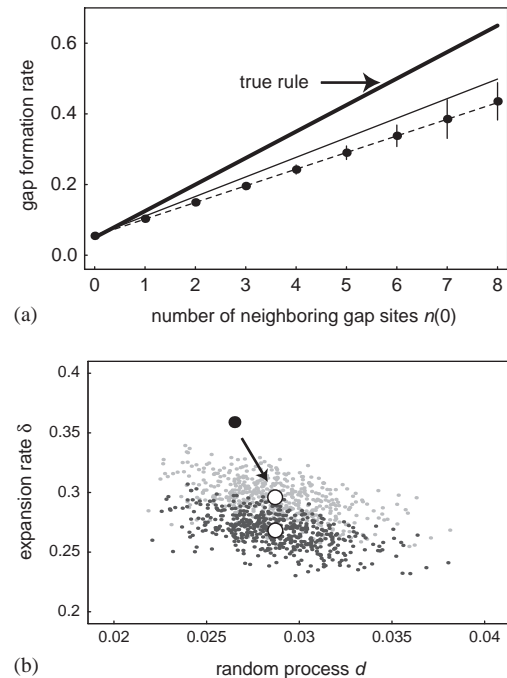


Fig. 3. The bias in estimating parameters. (a) The true parameters and biased estimators. We fixed true parameters as $(d, \delta, b, \beta) = (0.050, 0.60, 0.050, 0.60)$. We generated a 500 spatial data using the model, and then calculated approximate maximum likelihood estimates for each data. A solid line, $y = (0.60/8)n(0) + 0.050$, gives the true gap formation rule used to simulate the model. Solid circles and vertical lines are the mean and standard error of the fraction of non-gap sites that experienced transition to gap sites within a year. A dashed line, $y = (0.38/8)n(0) + 0.055$, is the mean of the approximate maximum likelihood estimates. The difference between the true and estimated rule indicates considerable bias included in the estimate. It overestimates an independent rate d (intercept of the line) and underestimates the expansion rate δ (slope of the line). The thin straight line is the estimated rule in which the bias caused by the neglect of the difference between the instantaneous rate and fraction of transitions per year was removed. (b) $\delta - d$ plane. We generated 500 independent replicates of spatial data using parameters, $(d, \delta, b, \beta) = (0.027, 0.36, 0.043, 0.36)$, and then computed the approximate maximum likelihood estimates for each data. A solid circle indicates the true set of parameters for gap formation (d, δ). Dots in a black color are the approximate maximum likelihood estimates of 500 replicates, the mean of which is indicated by an open circle. Dots in gray color are the modified estimates—the bias was partially removed by considering the difference between the instantaneous rate and fraction of transitions per year.

2.2.1. Two reasons for the bias

There are two dominant reasons for the bias. The first is the neglect of the difference between the instantaneous transition rate and the fraction of sites experiencing a transition in a finite time interval. Since the gap formation occurs throughout the year, we adopted a continuous-time Markov model for the forest gap dynamics. The observation is, however, made once per year, and hence the fraction of sites that experienced transition within a year is not exactly the same as the instantaneous transition rate (if the transition rate is very small, they are approximately the same, but this is

not to be the case in this study). If the instantaneous transition rate is r , the fraction of sites undergoing transition per year is $1 - \exp[-r]$. Using this relationship, we can convert the observed fraction of transitions to the instantaneous rate of transition by a simple method (Appendix A). In Fig. 3a, a thin solid line indicates the estimate of transition rate considering this source of bias. It is less biased than the approximate likelihood estimates without this modification. In Fig. 3b, the modified estimates are indicated by gray dots with their average (an open circle), which are closer to the “true” transition parameters than the estimates without modification. Hence, the difference between the instantaneous transition rate and fraction of transitions per year partially explains the cause of bias. However, there still remains a large bias between the true transition parameters and the estimates (Fig. 3).

The second source of the bias is illustrated in Fig. 4. In Fig. 4, we assumed that three non-gap sites have changed to gap sites within a year. Since each of these newly formed gap sites have no neighboring gap site in the beginning of year t , the approximate maximum likelihood method regards that these three gap formations have occurred at a rate of d and were independent of δ (top figure in Fig. 4). However in the continuous-time model, three transitions may have occurred one by one generating a “chain” of transitions (bottom figure in Fig. 4). The gap formation rate is enhanced by a gap expansion of neighboring gap sites. For example, the second transition occurs at a rate of $d + \delta/8$ instead of d because it has one neighboring gap site. The third transition occurs at a rate of $d + 2\delta/8$ because it has two gaps in the neighborhood. We cannot observe this chain reaction of gap expansion from the data, but in a proper treatment, the observed transitions should be counted as the realization of both neighbor-independent gap formation (d) and gap expansion (δ).

The problem in simple regression method is due to the assumption of independence between different transitions occurring within a single census interval. This assumption may be valid if the time interval is sufficiently short (observations are frequent enough) and only one transition at local scales is observed between two observations. However, comparing map data observed at two consecutive times, we often see multiple transitions occurring at local scales. We plot the fraction of gap formation events along the number of adjacent sites undergoing gap formation (Fig. 5). The result shows that multiple gap formations in the neighborhood occurred frequently, though the formation of large gaps was less frequent. There is a similar bias in estimating the gap closure rate. Again there is a significant bias—underestimation of neighbor-dependent rate (β) and overestimation of neighbor-independent rate (b). In general, this sort of bias arises when the data are collected at discrete points in time but the underlying process is continuous.

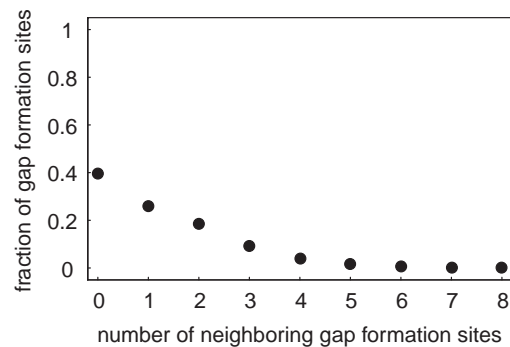


Fig. 5. Fraction of gap formation events according to the number of adjacent sites undergoing gap formation. Solid circles represent the fraction of non-gap sites that experienced transition to gap sites in two consecutive years, 1983 and 1984.

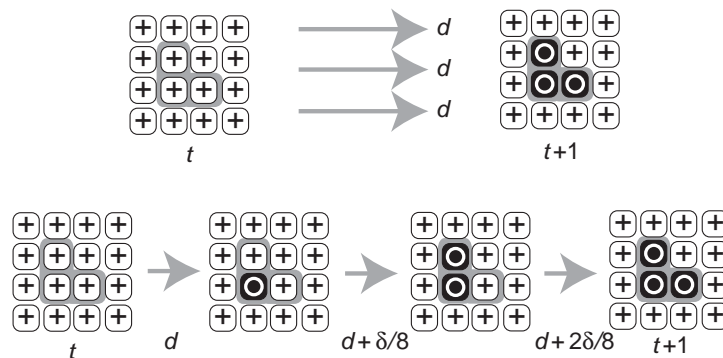


Fig. 4. Mechanism generating the bias. Bias is caused by multiple transitions occurred in the neighborhood within a single census interval. Three non-gap (+) sites experienced the transition to gap (0) sites within a year (above figure). All of these sites had no gaps in their neighbors in the beginning of the year. Hence, the approximate maximum likelihood method regards these three gap formations have occurred at a rate of d . However, three transitions may occur one by one (bottom figure): the second transition occurs at a rate of $d + \delta/8$, and the third transition occurs at a rate of $d + 2\delta/8$. The neglect of enhancement of the transition rate causes the underestimate of expansion rate, δ . Moore neighborhood is adopted ($z = 8$).

In principle we can construct the maximum likelihood estimate considering interrelated transitions within a single census interval. For example, in the case illustrated in Fig. 4, it may be possible to construct the likelihood function for this particular sequence of three transition events. In general cases, however, there are many pathways to reach the final spatial pattern. To implement proper maximum likelihood calculation, we need to consider all the possible pathways and evaluate the transition probability along each, which would be a formidable task and is not practical to perform in this study.

This difficulty might be overcome by applying Monte Carlo (MC) (Gibson and Austin, 1996) or Markov chain Monte Carlo (MCMC) (Gibson, 1997) methods, which are used for parameter estimation of the stochastic spatial model of disease spread. Both methods simulate a large number of the unobserved pathways of infections between two observation times to estimate the likelihood function of the parameter. When N sites are newly infected between two observations, there are $N!$ possible pathways of infections. If we can make a suitable sampling of pathways, the likelihood of the parameter can be given as a marginal density of the parameter numerically computed by averaging the conditional likelihood with respect to all sampled pathways (Gelfand and Smith, 1990). To estimate the likelihood, the MC method considers that each particular ordering of infection is selected with the same probability, $1/N!$. The MCMC method samples a pair of parameter and infection ordering from Markov chain whose stationary distribution is the relative value of the likelihood.

When these methods are applied to our model, they will give the approximate likelihood rather than the exact value. The estimated approximate likelihood value is close to the true value when the transition rate is small enough not to induce multiple transitions at the same site between two observations. If the model incorporates only single transition process (for example disease infection), multiple transitions at the same site do not happen—each site experiences either a single or no transition. Thus, the possible number of pathways of transition is consistent to $N!$. However, when the model incorporates two (or multiple) transition processes (for example recovering from infection), the same site may experience two or more transitions within an observation interval—this is especially so if the transition rate is large. In this case, we cannot construct possible transition pathways simply by making the ordering of observed transitions. The number of possible pathways is larger than $N!$, meaning that sampling of pathways from $N!$ orderings may produce the bias in the estimate. The gap dynamics model includes two processes: a “gap expansion” and a “gap closure”. Thus there is a possibility that the model may produce a sequence of

transitions at the same site within a single census interval (for example, two transitions from a gap to a non-gap, and a non-gap to a gap), though such multiple events at the same site are rare. Estimating the likelihood incorporating these multiple transitions is, again, a formidable task and may not be plausible for a practical purpose.

2.3. Monte Carlo bias correction

The Monte Carlo bias correction (MCBC) developed by Hakoyama and Iwasa (2000a,b) is a computationally intensive, but reasonable method to remove the bias due to correlated transitions. Consider a general problem in estimating a parameter θ of a model using a biased estimator. Suppose S is the continuous random variable represented by a probability density function, $f(s|\theta)$. Let $\hat{\theta}(s)$ be a biased estimate of θ calculated from observed realization s . We can generate a significantly large number of independent realizations s^* by a direct Monte Carlo simulation of the model with a given parameter value of θ , and then calculate $\hat{\theta}(s^*)$ for each s^* . Let $\hat{E}[\hat{\theta}(s^*)|\theta]$ be the arithmetic average of $\hat{\theta}(s^*)$ for a given parameter θ . Since the estimator is biased, $\hat{E}[\hat{\theta}(s^*)|\theta]$ is different from the true parameter θ (as shown in Fig. 3). The Monte Carlo bias-corrected estimate $\hat{\theta}_{bc}(s)$, is the one that satisfies the following equality for a given value of $\hat{\theta}(s)$:

$$\hat{E}[\hat{\theta}(s^*)|\hat{\theta}_{bc}(s)] = \hat{\theta}(s). \quad (2)$$

Thus, the $\hat{\theta}_{bc}(s)$ is the parameter values for which the average of the biased estimates over many simulated realizations is equal to the biased estimate from the observed realization, $\hat{\theta}(s)$ (Appendix B).

If the expected value of the biased estimator, $\hat{\theta}(S)$, given by $E[\hat{\theta}(S)|\theta]$, is a monotonic function of θ , the bias corrected estimator exists and is unique. The bias corrected estimator is unbiased if θ is a linear function of $E[\hat{\theta}(S)|\theta]$. A linear relationship between θ and $E[\hat{\theta}(S)|\theta]$ is a reasonable assumption when the variance of the $\hat{\theta}(S)$ is small or when the relation itself is linear (Hakoyama and Iwasa, 2000a,b; Appendix B). We can examine the magnitude of bias in the bias-corrected estimator itself by the same sequence of procedures explained above: choosing a true parameter, generating a number of Monte Carlo data by the computer simulation of the model with a true parameter, and calculating the bias-corrected estimates for each data. The bias-corrected estimates will be scattered around the true parameter, with their mean values close to the true parameter. The study of a stochastic population dynamics with density-dependent showed this property by applying parameters estimated from the time series data (Hakoyama and Iwasa, 2000a,b).

To search for $\hat{\theta}_{bc}(s)$ that satisfies Eq. (2), an iterative procedure was proposed (Hakoyama and Iwasa,

2000a,b; Appendix C). The procedure appeared to be very efficient. For parameter values we examined ($d = b = 0.02$, $0.2 \leq \delta$, $\beta \leq 1.0$), the biased estimates converged to the unbiased estimates in 3–11 steps. When the magnitude of bias, x , is simply measured as Euclidian distance between true values and biased estimates, convergence steps required to remove the bias, y , linearly increased as the bias increased ($y = 19x + 2.5$, $r^2 = 0.96$).

We have illustrated the MCBC method using a simple model involving only a single parameter. The technique can be easily applied to more highly parameterized models. In the forest gap dynamics, as discussed in the next section, the parameter θ to be estimated is a set of rate parameters: (d, δ) for gap formation and (b, β) for gap closure.

3. Application and results

3.1. Gap dynamics of the 50 ha plot in Barro Colorado Island

We applied the MCBC method to estimate parameter values by fitting the model to a temporal sequence of canopy–gap data observed at the permanent plot in Barro Colorado Island (BCI). The map data were provided over 11 years from 1983 to 1993, and each map includes 101 by 201 sites that are either “gap” (0) (< 20 m) or “non-gap” sites (+) (≥ 20 m) depending on the vegetation height. The sites which made transitions between two observation times are classified according to the number of neighboring gap sites (Fig. 2). We estimated gap formation rates ($\hat{d}(m), \hat{\delta}(m)$) and gap closure rates ($\hat{b}(m), \hat{\beta}(m)$) from a pair of spatial data observed at two consecutive years ($1983 \leq m \leq 1992$) using the approximate maximum likelihood method explained in Eq. (A.1) in Appendix A (Fig. 6). The corrected-approximate maximum likelihood estimates (Eq. (A.2)) were similarly calculated, but we do not show the results because resultant bias-corrected estimates by MCBC were the same between the two.

We performed Monte Carlo simulations of the model with the estimated parameters ($\hat{d}(m), \hat{\delta}(m), \hat{b}(m), \hat{\beta}(m)$), and compared the spatial patterns generated in the simulated runs to the observed patterns. As an initial condition for each run, we used the map data observed in 1983 at the BCI plot. To characterize the spatial patterns, we calculated two statistics: the global density ρ_0 and the local density $q_{0/0}$ of gaps (Harada and Iwasa, 1994). ρ_0 is the average density of gap sites. In contrast, $q_{0/0}$ is the conditional probability that a randomly chosen neighbor of a gap site is also a gap. If the spatial distribution of gap sites is aggregated, rather than random, the local gap density is larger than the global gap density (i.e. $q_{0/0} > \rho_0$).

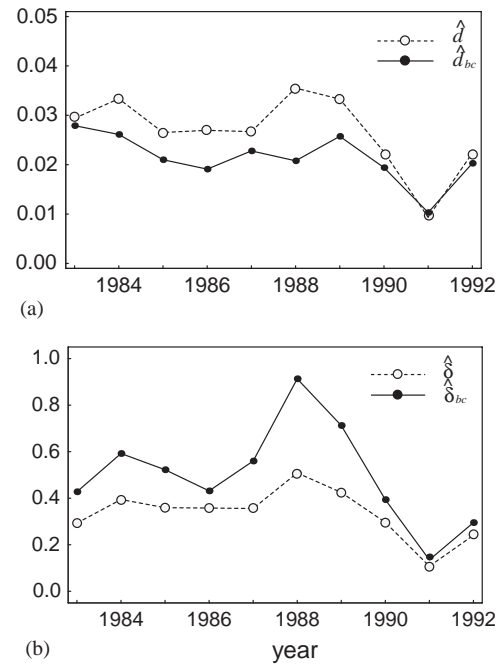


Fig. 6. Biased and bias-corrected gap formation rates estimated from BCI canopy data. Each estimate was calculated from a pair of data observed in two consecutive years. (a) Estimates of the independent rate. A broken line and open circles are the biased estimate, \hat{d} , and a solid line and solid circles are bias-corrected estimates, \hat{d}_{bc} . (b) Estimates of the expansion rate. A broken line and open circles are biased estimates, $\hat{\delta}$, and a solid line and solid circles are bias-corrected estimates, $\hat{\delta}_{bc}$.

Fig. 7 gives the resultant global and local gap densities from the simulated runs. Local gap density, $q_{0/0}$, declined in both cases with the Neumann neighborhood ($z = 4$, Fig. 7a) and with the Moore neighborhood ($z = 8$, Fig. 7b) as shown by dashed lines. However, the global gap density ρ_0 was almost constant (thin solid lines in Fig. 7). Thus, $q_{0/0}$, gradually approaches ρ_0 , implying that the spatial gap distribution becomes less clumped with time. However, observed values of ρ_0 and $q_{0/0}$ at the BCI plot were more or less stationary, without showing a clear decline (open circles in Fig. 7). If the model is accurate in describing the gap dynamics at the BCI plot, and if the parameter estimation is done correctly, a series of spatial patterns generated in the simulated runs should be similar to the observed one. However, this did not seem to be the case.

3.1.1. Bias-corrected estimates

The discrepancy between the model's prediction and the observed data is partially caused by the bias in parameter estimation. We applied MCBC to remove the bias included in the approximate maximum likelihood estimates, ($\hat{d}(m), \hat{\delta}(m), \hat{b}(m), \hat{\beta}(m)$), and then obtained bias-corrected estimates, ($\hat{d}_{bc}(m), \hat{\delta}_{bc}(m), \hat{b}_{bc}(m), \hat{\beta}_{bc}(m)$), shown in Fig. 6. The bias-corrected estimates of

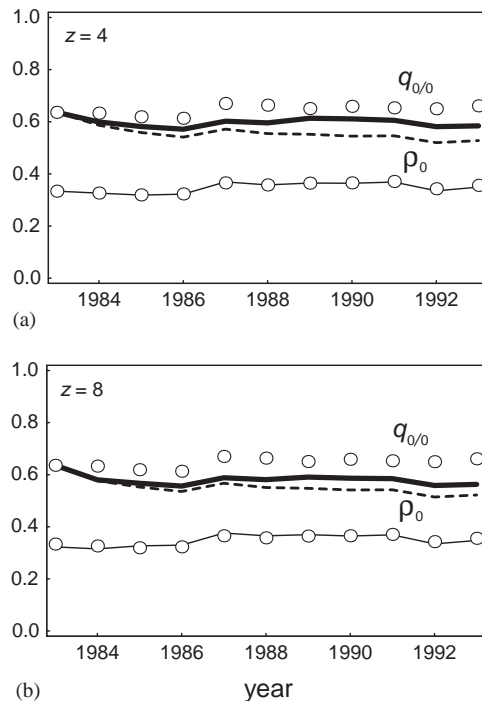


Fig. 7. The global gap density, ρ_0 , and the local gap density, $q_{0/0}$. Open circles are observed values calculated from the BCI data. Predicted ρ_0 by applying biased and bias-corrected estimates are illustrated as thin solid lines. Dashed lines are predicted $q_{0/0}$ with the biased estimates. Thick solid lines are predicted $q_{0/0}$ with bias-corrected estimates. (a) Neumann neighborhood (number of neighboring site, $z = 4$). (b) Moore neighborhood ($z = 8$).

neighbor-independent rate for gap formation, $\hat{d}_{bc}(m)$, were smaller than the biased estimates, $\hat{d}(m)$, whilst the bias-corrected estimates of neighbor-dependent rate, $\hat{\delta}_{bc}(m)$, were larger than the biased estimates, $\hat{\delta}(m)$. The difference between bias-corrected and biased estimates was very small in 1991, which is presumably explained by a small number of aggregated transitions occurred in that interval.

We performed computer simulations of the model using the bias-corrected estimates, $(\hat{d}_{bc}(m), \hat{\delta}_{bc}(m), \hat{b}_{bc}(m), \hat{\beta}_{bc}(m))$. The spatial patterns generated by simulations with the bias-corrected estimates were closer to the observed patterns for both Neumann (Fig. 7a) and Moore neighborhood (Fig. 7b). Thus applying the Monte Carlo bias correction (MCBC), the inconsistency between the model's prediction and the observation was improved. Neumann neighborhood showed a better fit to the data than Moore neighborhood (the sum of squared difference of $q_{0/0}$ between model's prediction and the data was 0.0049 for Neumann neighborhood, and 0.027 for Moore neighborhood). This suggests that the interaction between nearest neighbors might be more important than those between non-nearest neighbors.

4. Discussion

We pointed out a general problem in estimating parameters of continuous-time spatially explicit models from a temporal sequence of map data observed at discrete times. We illustrated the problem by fitting a model to the data of canopy–gap maps observed at the 50 ha plot in Barro Colorado Island. The simple linear regression or the approximate maximum likelihood method is valid if sampling is frequent and only a few transitions are observed within a single census interval. However, this assumption is inappropriate to describe the forest gap dynamics we studied in the paper, because transitions are locally correlated—one tree-fall may make surrounding trees unstable and further enhance the tree-fall rate (Fig. 4). When a long chain of gap expansion (or canopy expansion) is created by short-range interaction between sites, the assumption of independent transition results in underestimation of the neighbor-dependent rate and an overestimation of the neighbor-independent rate.

Both in temperate and in tropical forests, gap formation occurs all the year round (Denslow, 1987; Runkle, 1989), which suggests that a continuous-time model would be more realistic for the forest gap dynamics than a discrete-time model where a clear seasonality in gap formation is assumed. However, if we use a continuous-time model, we must overcome the difficulty in estimating the rate parameters of the model from a temporal sequence of spatial data observed at discrete times. Even if transitions at different sites within an infinitesimally short time interval is independent, the transitions within a period of finite length (say 1 year) are no longer independent. Such interrelated transitions require consideration of all the possible pathways of transition to construct an exact likelihood. In contrast, the approximate estimates such as Eqs. (A.1) and (A.2) assuming independent transitions are simple enough to be applied but include a considerable bias.

In this study, we applied a computer intensive method abbreviated as MCBC (Hakoyama and Iwasa, 2000a,b) to eliminate the bias. The idea is straightforward. Given an observed sample s and a simulation model, the bias-corrected estimates are the parameter set for which the average of the biased estimates computed from many Monte Carlo simulations of the model is equal to the biased estimates obtained from s (Eq. (2)). An iteration procedure to search for the bias-corrected estimates (Hakoyama and Iwasa, 2000a,b; Appendix C) results in very quick convergence. The technique is applicable to any system for which we can perform computer simulations, and any data observed at discrete intervals such as every year or every 5 years. Hence, we believe MCBC is broadly useful in spatial ecology. Alternative approach is a modification of the Markov Chain Monte Carlo (MCMC) method studied by

Gibson (1997), which will be an interesting challenge for future study.

4.1. Tropical seasonal forest dynamics

We illustrated the MCBC method by fitting the continuous-time Markov model (Kubo et al., 1996) to the gap dynamics data observed at the BCI plot. There are several interrelated theoretical works for forest gap dynamics. Katori et al. (1998) modified the model proposed by Kubo et al. (1996) by assuming that the transition rate increases exponentially with the number of neighboring gap sites instead of linearly. Katori et al. (1998) proved that spatial patterns at the stationary probability distribution generated by the model is mathematically equivalent to a random sample from the ensemble of spatial patterns generated by the Ising model with magnetic field. The Ising model is one of the most intensively studied models in physics and it is well known that the cluster size distribution follows a power function (appearing as a straight line on the log–log plot) when the model is near the critical point (Katori et al., 1998). Katori et al. (1998) and Kizaki and Katori (1999) showed that the model generates spatial patterns that nicely approximate the real gap-size distribution including gaps of large size, implying that the nearest-neighbor interaction can potentially cause a long-range correlation.

The cellular automaton (the “forest game”) was also adopted as a forest growth model for the gap dynamics at the BCI forest (Solé and Manrubia, 1995; Manrubia and Solé, 1997). Manrubia and Solé (1997) pointed out that the local gap density $q_{0/0}$, and the gap size distributions fitted to the observed pattern were different from the equilibrium distribution of the model studied by Kubo et al. (1996). The study in the present paper suggests that the deviation is, at least partially, caused by the underestimation of the strength of interaction between neighboring sites.

The inconsistency between the model’s prediction and the observation was improved by applying the MCBC (Fig. 7). However, the expected value of the local gap density with MCBC is still lower than that observed (Fig. 7). This remaining discrepancy may result from the assumption of short-range interaction between sites. It is likely that the interaction between sites occurs at a broader spatial scale than the nearest neighbor (Manrubia and Solé, 1997), and such a long-range interaction would generate more aggregated gap distribution. The inability to explain the observed pattern may also come from the assumption that gap dynamics occur at the $5 \times 5 \text{ m}^2$ spatial scale. Gap formation occurring at larger scales or at multiple scales may be more biologically appropriate. In addition, spatial heterogeneity of geographical gradients, nutrient distribution, and groundwater level may influence the forest gap

dynamics in the BCI forest. Careful statistical data analysis of forest gap dynamics may identify the need to incorporate further aspects into the model.

Acknowledgements

This work was supported in part by a grant-in-aid from the Ministry of Education, Science, Sports, and Culture, Japan and Japan Society for the Promotion of Science (JSPS). We thank the following people: O. N. Bjørnstad, B. Bolker, H. Caswell, M. Ferrari, A. Hastings, M. Katori, S. Kizaki, T. Kohyama, T. Kubo, R. Law, S. A. Levin, T. Nakashizuka, and A. Sasaki, for their useful comments.

Appendix A. Approximate maximum likelihood estimates of rate constants

Transition rates (d, δ, b, β) were estimated from the 10 pairs of map data of canopy height sampled at two consecutive years: (1983, 1984), ..., (1992, 1993). For each pair, let $L(x)$ be the number of non-gap sites with x gap neighbors and $N(x)$ be the number of non-gap sites that made transition to gap sites within a year. The likelihood for gap formation rate (d, δ) is

$$f_1(d, \delta) = \prod_{x=0}^z \binom{L(x)}{N(x)} \left(d + \frac{\delta}{z}x \right)^{N(x)} \times \left(1 - d - \frac{\delta}{z}x \right)^{L(x)-N(x)}, \quad (\text{A.1})$$

where z is the number of neighboring sites ($z = 4$ with Neumann neighborhood and $z = 8$ with Moore neighborhood). The pair of parameters ($\hat{d}, \hat{\delta}$) that maximizes $f_1(d, \delta)$ is easily obtained by calculating the derivative of $\log[f_1(d, \delta)]$ and then setting it equal to zero. We call this the approximate maximum likelihood estimate, in which the transitions of different sites were assumed to be independent. Gap closure rates ($\hat{b}, \hat{\beta}$) were calculated in the same way.

This estimate includes a strong bias (Fig. 3). One source of bias is the neglect of the distinction between the instantaneous rate of transition and the fraction of sites that experienced transition in a year. If the instantaneous rate is r , the observed fraction of sites that show transition per year is $1 - \exp[-r]$, and the fraction of sites that do not show transition is $\exp[-r]$. By setting $r = d + (\delta/z)n(0)$, the expected fraction of sites showing transition is $1 - \exp[-d - (\delta/z)n(0)]$, and the rate in Eq. (A.1) should be replaced accordingly.

Then the likelihood is now

$$f_2(d, \delta) = \prod_{x=0}^z \binom{L(x)}{N(x)} \left(1 - \exp\left[-d - \frac{\delta}{z}x\right]\right)^{N(x)} \times \left(\exp\left[-d - \frac{\delta}{z}x\right]\right)^{L(x)-N(x)}. \quad (\text{A.2})$$

The pair of parameters (d, δ) that maximize $f_2(d, \delta)$ are the estimates indicated by a thin line in Fig. 3a, and gray dots in Fig. 3b.

Appendix B. The Hakoyama–Iwasa’s Monte Carlo bias correction

Hakoyama and Iwasa (2000a,b) proved that the bias-corrected estimators given in Eq. (2) in the text are close to the unbiased estimators. Here we summarize the result.

We consider a simple problem in estimating a parameter θ of a parametric model involving a single parameter. Let $f(s|\theta)$ be the probability density function specified by the model, which represents the continuous random variable S^θ . To give a clear explanation, we specify the variable following the model with a given parameter value of θ as S^θ that is simply represented by S in the text. Suppose the estimator, $\hat{\theta}(S^\theta)$, is a function of S^θ and denote the estimate computed from a sample s as $\hat{\theta}(s)$. The expected value of the estimator is given by

$$E[\hat{\theta}(S^\theta)|\theta] = \int \hat{\theta}(s)f(s|\theta) ds. \quad (\text{B.1})$$

If the estimator, $\hat{\theta}(S^\theta)$, is unbiased,

$$E[\hat{\theta}(S^\theta)|\theta] = \theta. \quad (\text{B.2})$$

However, the estimator in question in the current study includes the bias. Here, we explain how the bias is removed and show the bias-corrected estimator, $\hat{\theta}_{bc}(S^\theta)$, is approximately the unbiased estimator when the variance of the biased estimator is small, or when θ is a linear function of the biased estimator.

To make the discussion clear, we denote the biased estimator as $\hat{\theta}_{bias}(S^\theta)$. Assume that the true parameter θ is the smooth and monotonic function of the expected value of the biased estimator,

$$\theta = h(E[\hat{\theta}_{bias}(S^\theta)|\theta]). \quad (\text{B.3})$$

If $h(*)$ can be approximated as a linear function

$$\theta = E[h(\hat{\theta}_{bias}(S^\theta))|\theta]. \quad (\text{B.4})$$

Comparing Eqs. (B.2) and (B.4), $h(\hat{\theta}_{bias}(S^\theta))$ is an approximately unbiased estimator, which is a bias corrected estimator, $\hat{\theta}_{bc}(S^\theta)$, we want to obtain. Hence we define,

$$h(\hat{\theta}_{bias}(S^\theta)) = \hat{\theta}_{bc}(S^\theta). \quad (\text{B.5})$$

If θ is substituted by $\hat{\theta}_{bc}(S^\theta)$, Eq. (B.4) becomes

$$\hat{\theta}_{bc}(S^\theta) = h(E[\hat{\theta}_{bias}(S^{\hat{\theta}_{bc}})|\hat{\theta}_{bc}(S^\theta)]), \quad (\text{B.6})$$

where $S^{\hat{\theta}_{bc}}$ is the random variable following the model with a given parameter $\hat{\theta}_{bc}(S^\theta)$. Applying the inverse function of $h(*)$ to Eqs. (B.5) and (B.6), we have,

$$E[\hat{\theta}_{bias}(S^{\hat{\theta}_{bc}})|\hat{\theta}_{bc}(S^\theta)] = \hat{\theta}_{bias}(S^\theta). \quad (\text{B.7})$$

Eq. (B.7) means that we can remove the bias if we obtain $\hat{\theta}_{bc}(S^\theta)$ satisfying the above condition.

We calculate the expected value of $\theta(S^\theta)$ using the following procedure: (1) we chose a parameter value of θ , (2) under a given parameter value, we generate a significantly large number of data s^* by independent Monte Carlo simulations of the model. (3) we calculate the estimate, $\hat{\theta}(s^*)$, for each s^* , and take the arithmetic average of these values. When enough number of s^* is generated, the average of $\hat{\theta}(s^*)$ denoted by $\hat{E}[\hat{\theta}(s^*)|\theta]$ asymptotically equals to the $E[\hat{\theta}(S^\theta)|\theta]$. Bias corrected estimator computed by this Monte Carlo procedure is “Monte Carlo bias corrected estimator” given in Eq. (2) in the text.

Eq. (B.7) stands upon the assumption that $h(*)$ can be approximated as a linear function. This assumption is valid when the biased estimator, $\hat{\theta}_{bias}(S^\theta)$, has a small variance or when $h(*)$ itself is a linear function. To show this, we performed Taylor expansion of $h(\hat{\theta}_{bias}(S^\theta))$ around $\bar{\theta} = E[\hat{\theta}_{bias}(S^\theta)|\theta]$, and obtain

$$\begin{aligned} h(\hat{\theta}_{bias}(S^\theta)) &= h(\bar{\theta}) + (\hat{\theta}_{bias}(S^\theta) - \bar{\theta})h'(\bar{\theta}) \\ &\quad + \frac{1}{2}(\hat{\theta}_{bias}(S^\theta) - \bar{\theta})^2h''(\bar{\theta}) \\ &\quad + [\text{higher order terms}]. \end{aligned} \quad (\text{B.8})$$

Expected value of $h(\hat{\theta}_{bias}(S^\theta))$ is now given by calculating the conditional average with respect to S^θ ,

$$\begin{aligned} E[h(\hat{\theta}_{bias}(S^\theta))|\theta] &= h(\bar{\theta}) + \frac{1}{2} \text{Var}[\hat{\theta}_{bias}(S^\theta)|\theta]h''(\bar{\theta}) \\ &\quad + [\text{higher order terms}]. \end{aligned} \quad (\text{B.9})$$

Eq. (B.8) means that if the variance of the biased estimator is small, the assumption of linear relationship between the true value, θ , and the biased estimator, $\hat{\theta}_{bias}(S^\theta)$, is valid, and thus the bias-corrected estimator, $\hat{\theta}_{bc}(S^\theta)$, is approximately the unbiased estimator.

Appendix C. Iteration procedure for the Hakoyama–Iwasa’s Monte Carlo bias correction

Let $\hat{\mathbf{P}}_{obs} = (\hat{d}_{obs}, \hat{\delta}_{obs}, \hat{b}_{obs}, \hat{\beta}_{obs})^T$ be the approximate maximum likelihood estimates calculated from an observed spatial pattern. Assume that $\hat{\mathbf{P}}_{obs}$ includes a significant bias. We generate many independent Monte Carlo data by the model with $\hat{\mathbf{P}}_{obs}$ and calculate the maximum likelihood estimate $(\hat{d}^*, \hat{\delta}^*, \hat{b}^*, \hat{\beta}^*)$ for each. The average of these values, denoted by $(\hat{E}[d^*|\hat{\mathbf{P}}_{obs}], \hat{E}[\delta^*|\hat{\mathbf{P}}_{obs}], \hat{E}[b^*|\hat{\mathbf{P}}_{obs}], \hat{E}[\beta^*|\hat{\mathbf{P}}_{obs}])$, are different from

$\hat{\mathbf{P}}_{obs}$, because the estimates are biased. Fig. 3 indicates the overestimation of d ($\hat{E}[\hat{d}^*|\hat{\mathbf{P}}_{obs}] > \hat{d}_{obs}$) and the underestimation of δ ($\hat{E}[\hat{\delta}^*|\hat{\mathbf{P}}_{obs}] < \hat{\delta}_{obs}$). We have similar biases in estimating gap closure rate ($\hat{E}[\hat{b}^*|\hat{\mathbf{P}}_{obs}] > \hat{b}_{obs}$ and $\hat{E}[\hat{\beta}^*|\hat{\mathbf{P}}_{obs}] < \hat{\beta}_{obs}$). To reduce the bias, we search for the bias-corrected estimator $\hat{\mathbf{P}}_{bc}$ that satisfies Eq. (2) in the text as follows. Let $\hat{\mathbf{P}}_i = (\hat{d}_i, \hat{\delta}_i, \hat{b}_i, \hat{\beta}_i)^T$ be the sequence of rate parameters. Fixing $\hat{\mathbf{P}}_0$ as $\hat{\mathbf{P}}_{obs}$ in our first calculation, we iterate the following procedure:

$$\begin{aligned}\hat{d}_{n+1} &= \frac{\hat{d}_{obs}}{\hat{E}[\hat{d}^*|\hat{\mathbf{P}}_n]} \hat{d}_n, & \hat{\delta}_{n+1} &= \frac{\hat{\delta}_{obs}}{\hat{E}[\hat{\delta}^*|\hat{\mathbf{P}}_n]} \hat{\delta}_n, \\ \hat{b}_{n+1} &= \frac{\hat{b}_{obs}}{\hat{E}[\hat{b}^*|\hat{\mathbf{P}}_n]} \hat{b}_n, \\ \hat{\beta}_{n+1} &= \frac{\hat{\beta}_{obs}}{\hat{E}[\hat{\beta}^*|\hat{\mathbf{P}}_n]} \hat{\beta}_n \quad n = 1, 2, 3, \dots\end{aligned}\quad (C.1)$$

After several iterations, $\hat{\mathbf{P}}_{n+1}$ becomes close to $\hat{\mathbf{P}}_n$. When Eq. (C.1) converges, it is the bias-corrected estimator, $\hat{\mathbf{P}}_{bc}$, that satisfies

$$\begin{aligned}(\hat{E}[\hat{d}^*|\hat{\mathbf{P}}_{bc}], \hat{E}[\hat{\delta}^*|\hat{\mathbf{P}}_{bc}], \hat{E}[\hat{b}^*|\hat{\mathbf{P}}_{bc}], \hat{E}[\hat{\beta}^*|\hat{\mathbf{P}}_{bc}])^T \\ \approx (\hat{d}_{obs}, \hat{\delta}_{obs}, \hat{b}_{obs}, \hat{\beta}_{obs})^T.\end{aligned}\quad (C.2)$$

References

- Alonso, D., Solé, R.V., 2000. The divgame simulator: a stochastic cellular automata model of rainforest dynamics. *Ecol. Model.* 133, 131–141.
- Brokaw, N., Busing, R.T., 2000. Niche versus chance and tree diversity in forest gaps. *Trends Ecol. Evol.* 15, 183–188.
- Denslow, J.S., 1987. Tropical rain-forest gaps and tree species-diversity. *Annu. Rev. Ecol. Syst.* 18, 431–451.
- Dieckmann, U., Law, R., Metz, J.A.J., 2000. *The Geometry of Ecological Interaction: Simplifying Spatial Complexity*. Cambridge University Press, Cambridge.
- Gelfand, A.E., Smith, A.F.M., 1990. Sampling-based approaches to calculating marginal densities. *J. Am. Stat. Assoc.* 85, 398–409.
- Gibson, G.J., 1997. Markov chain Monte Carlo methods for fitting spatiotemporal stochastic models in plant epidemiology. *Appl. Stat.—J. Roy. Stat. Soc. C* 46, 215–233.
- Gibson, G.J., Austin, E.J., 1996. Fitting and testing spatio-temporal stochastic models with application in plant epidemiology. *Plant Pathol.* 45, 172–184.
- Grau, H.R., 2002. Scale-dependent relationships between treefalls and species richness in a neotropical montane forest. *Ecology* 83, 2591–2601.
- Hakoyama, H., Iwasa, Y., 2000a. Extinction risk of a density-dependent population estimated from a time series of population size. *J. Theor. Biol.* 204, 337–359.
- Hakoyama, H., Iwasa, Y., 2000b. Bias correction and confidence intervals for parametric models based on the Monte-Carlo sampling method. *Jpn. J. Biometrics* 20, 143–154.
- Harada, Y., Iwasa, Y., 1994. Lattice population dynamics for plants with dispersing seeds and vegetative propagation. *Res. Popul. Ecol.* 36, 237–249.
- Hubbell, S.P., Foster, R.B., 1986. Canopy gaps and the dynamics of a neotropical forest. In: Crawley, M.J. (Ed.), *Plant Ecology*. Blackwell, Oxford, pp. 77–96.
- Hubbell, S.P., Foster, R.B., O'Brien, S.T., Harms, K.E., Condit, R., Wechsler, B., Wright, S.J., de Lao, S.L., 1999. Light-cap disturbances, recruitment limitation, and tree diversity in a neotropical forest. *Science* 283, 554–557.
- Kanzaki, M., Yoda, K., Dhanmaonda, P., 1994. Mosaic structure and tree growth pattern in a monodominant tropical seasonal evergreen forest in Thailand. In: Peet, R.L., Box, E.O. (Eds.), *Vegetation Science in Forestry*. Kluwer Academic Publishers, Netherlands, pp. 499–517.
- Katori, M., Kizaki, S., Terui, S., Kubo, T., 1998. Forest dynamics with canopy gap expansion and stochastic Ising model. *Fractals* 6, 81–86.
- Kizaki, S., Katori, M., 1999. Analysis of canopy-gap structures of forests by Ising–Gibbs states—equilibrium and scaling property of real forests. *J. Phys. Soc. Jpn.* 68, 2553–2560.
- Kubo, T., Iwasa, Y., Furumoto, N., 1996. Forest spatial dynamics with gap expansion: total gap area and gap size distribution. *J. Theor. Biol.* 180, 229–246.
- Law, R., Herben, T., Dieckmann, U., 1997. Non-manipulative estimates of competition coefficients in a montane grassland community. *J. Ecol.* 85, 505–517.
- Lawton, R.O., Putz, F.E., 1988. Natural disturbance and gap-phase regeneration in a wind-exposed tropical cloud forest. *Ecology* 69, 764–777.
- Manrubia, S.C., Solé, R.V., 1997. On forest spatial dynamics with gap formation. *J. Theor. Biol.* 187, 159–164.
- Runkle, J.R., 1981. Gap regeneration in some old-growth forests of the eastern United States. *Ecology* 62, 1041–1051.
- Runkle, J.R., 1984. Development of woody vegetation in treefall gaps in a beech-sugar maple forest. *Hoarctic Ecol.* 7, 157–164.
- Runkle, J.R., 1989. Synchrony of regeneration, gaps, and latitudinal differences in tree species-diversity. *Ecology* 70, 546–547.
- Schnitzer, S.A., Carson, W.P., 2001. Treefall gaps and the maintenance of species diversity in a tropical forest. *Ecology* 82, 913–919.
- Schnitzer, S.A., Dalling, J.W., Carson, W.P., 2000. The impact of lianas on tree regeneration in tropical forest canopy gaps: evidence for an alternative pathway of gap-phase regeneration. *J. Ecol.* 88, 655–666.
- Solé, R.V., Manrubia, S.C., 1995. Are rainforests self-organized in a critical state? *J. Theor. Biol.* 173, 31–40.
- Yamamoto, S., 1993. Gap characteristics and gap regeneration in a subalpine coniferous forest on Mt. Ontake, Central Honshu. *Jpn. Ecol. Res.* 8, 277–285.